Title:
Design of Specialized Machining Equipment for Oral Implant Medical Devices

Authors:
Junren. Feng, jr.feng@siat.ac.cn, Shenzhen Institutes of Advanced Technology, Chinese Academy of Sciences.
Bo. Huang, bo.huang@siat.ac.cn, Shenzhen Institutes of Advanced Technology, Chinese Academy of Sciences.
Kai. He, kai.he@siat.ac.cn, Shenzhen Institutes of Advanced Technology, Chinese Academy of Sciences.
Xiaobing. Dang, xbdang@gzjanus.com, Guangdong Janus Biotechnology Co., Ltd.

Keywords:
Oral Implant Medical Devices, Design of Machine Tools, Rapid Generation of NC Processes, Compression of Helical Trajectories

DOI: 10.14733/cadconfP.2025.77-86

Introduction:

In the industry, manufacturers of oral implant medical device machining equipment are primarily concentrated in Europe and Japan. For efficiency, the CITIZEN L20 sliding head lathe is a representative model, capable of processing dozens of parts per minute with exceptional efficiency. However, it lacks versatility and cannot handle complex parts, as it is primarily designed for simple rotational components. For complex parts, Swiss companies such as Bumotec (S191H machining center) and Willemin-Macodel (408MT machining center) are the industry benchmarks. These machines offer high precision, compact structure, high automation, and excellent efficiency. However, their high costs—up to 6 million RMB per unit—place a significant financial burden on enterprises. In academia, research on machining equipment for oral implant medical devices remains limited. The Shenyang Northern Special Machine Tool Design Institute developed the CKD multifunctional CNC lathe for processing dental instruments like implants[1]. However, its functionality does not meet the requirements for machining diverse oral implant parts, and it has yet to achieve mass production. The Chinese University of Hong Kong developed a multi-axis CNC "turning-milling-gear hobbing" machining center specifically for the precision processing of small, complex parts like implants[2-4]. The machine has an automatic loading system and an automatic collection mechanism, which improves the automation level of the system.

In summary, there is currently a lack of specialized CNC machine tools for oral implant medical devices that are both functional and cost-effective. Therefore, this study focuses on developing a specialized machining equipment system for oral implant medical device components, such as implants and abutments. The aim is to enable efficient, full-process machining of serialized products in this category.

Development of Specialized Machining Equipment for Oral Implant Medical Devices:

As shown in Fig. 1, the development of this specialized machining equipment primarily involves three modules: machine tool structure design, machining process generation, and machining process control.

(1) Machine Tool Structure Design: This module focuses on the process characteristics of oral implant medical device components to determine the functional requirements of the machining equipment and design the structural components of the specialized equipment. To achieve better

control of machining accuracy, a spatial error model of the machine tool is established, and precision allocation is performed for key errors in the machine tool.

(2) Machining Process Generation: This module involves constructing machining process templates for serialized components such as implants and abutments and storing them in a process database. When a new component requires NC process planning, the system searches for a similar process template using a template-matching method. The associated machining processes from the matched template are then reused to generate the process plan for the new component.

(3) Machining Process Control: This module focuses on small components (e.g. implants) with machining trajectories primarily consisting of spatial arcs and helical lines. To reduce the data volume of NC codes and improve machining efficiency and quality, a spiral trajectory compression algorithm is employed. This algorithm smooths and compresses incoming small line segments, transforming the polyline machining path composed of numerous discrete segments into a smooth machining path. Additionally, to ensure smooth and continuous velocity transitions at corner transitions, the CNC system of the machine tool incorporates velocity lookahead control.

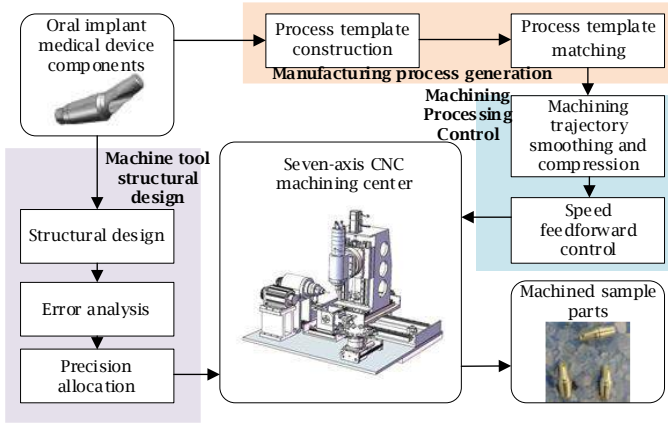

Fig. 1: Development process of specialized machining equipment.

Machine Tool Structure Design:

Process Analysis and Structural Design

In this study, the oral implant medical devices primarily consist of consumable parts such as dental implants with different diameter series and a universal abutment system, with some component designs shown in Fig. 2. Dental implants need to process conical threads, self-tapping blades, back inner holes, and inner hexagons. In addition to the aforementioned features, the universal abutment also requires the machining of inclined cylindrical surfaces at different angles. It can be seen that these parts have the characteristics of small sizes, numerous models, and complex processes.

For the machining of implants and abutments, the machining center needs to have not only turning, milling, drilling, thread milling, and cutting processes but also the ability to process multiple cutting angles and perform turning-milling compound operations. To achieve a higher level of automation, it should also be capable of back-side machining. Additionally, since different types of parts require different clamping methods, a modular design approach is necessary to facilitate fixture replacement for the machining of oral implant parts. Based on the above analysis, a specialized seven-axis turning-milling compound CNC machining center with a back-side machining device has been designed to achieve fully automated processing of oral implant medical device components. The structural diagram of the machining center is shown in Fig. 3.

(a) Dental Implants with Different Diameter Series

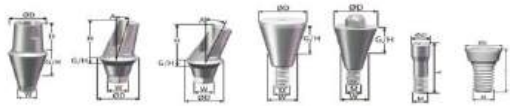

(b) Straight Abutments, Angled Abutments, Healing Abutments, etc.

Fig. 2: Oral implant medical device consumable parts (partial).

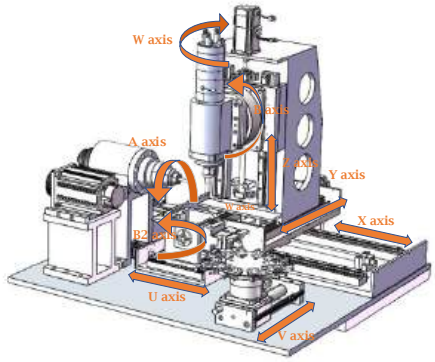

Fig. 3: Specialized seven-axis turning-milling compound CNC machining center.

The entire machine tool consists of seven axes and two cylinders. The rotary turning axis A and the linear axis X are fixed on the machine bed, while the linear axes Y and Z are mounted on the X axis. The rotary axis B is installed on the Z axis rail and can drive the milling spindle W axis for oscillating machining, enabling processes such as coaxial turning-milling and orthogonal turning-milling. The W axis can mount both turning tools and milling cutters, and it has a directional deadlock function to ensure the tool is securely fixed during turning operations. The linear axis V is parallel to the Y axis and controls the movement of the tool holder. The auxiliary processing device of the oral implant specialized machine tool is a linear axis U, parallel to the X axis, equipped with a precision vise. Under the action of the cylinder, the U axis can achieve a 90-degree rotation via the B2 axis. After the front-side machining of the part is completed, the U axis moves to the processed position, and the vise performs precise positioning and clamping. Once the spindle cuts the rod material, the cylinder drives the vise to rotate 90 degrees, cooperating with the spindle to complete the subsequent machining processes. In the machining of dental implant components, the milling spindle can freely switch between turning tools and milling cutters, enabling integrated mill-turn machining. The electric spindle combines the functions of the spindle and motor, achieving a "zero-transmission" system that overcomes the low speed, high vibration, and poor stability of traditional mechanical spindles. In this study, the DGZX-10030 milling electric spindle from GuangZhou HaoZhi Industrial Co. was selected. With high speed, high precision, and high rigidity, it is ideal for high-speed turning, milling, and grinding of both metallic and non-metallic materials.

Error Analysis

Accuracy is an important indicator for evaluating machine tool performance. Throughout the entire development process of the machine tool, the main approach to improving its accuracy is by reducing

errors. This paper primarily analyzes the sources of geometric errors in the dental implant machine tool and establishes a spatial error model for the machine tool.

The machine tool can be considered as consisting of multiple motion chains, including the bed, motion axes, tools, and workpieces. The relationships between rigid bodies are represented using a topological structure. The topological structure of the machine tool is shown in Fig. 4.

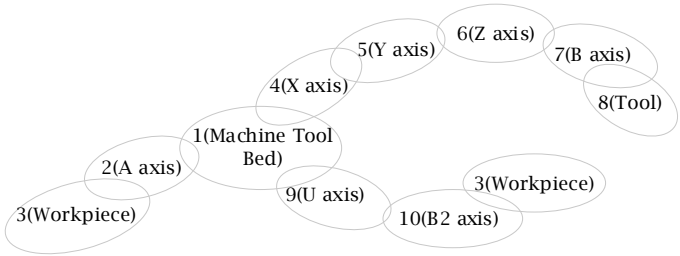

Fig. 4: Topological structure diagram of the machine tool.

Using the method of homogeneous coordinate transformation, the transformation matrix between two coordinate systems can be represented as Eqn. (1)., where A, B, C, X, Y, and Z represent the distances moved along the coordinate axes and the angles of rotation around the coordinate axes, respectively.

$$T = \begin{pmatrix} \cos B\cos C & -\cos B\sin C & \sin B & x \\ \cos A\sin C + \cos C\sin A\sin B & \cos A\cos C - \sin A\sin B\sin C & -\sin A\cos B & y \\ \sin A\sin C - \cos A\cos C\sin B & \cos C\sin A + \cos A\sin B\sin C & \cos A\cos B & z \\ 0 & 0 & 0 & 1 \end{pmatrix} \quad (1)$$

In the absence of errors, the ideal transformation matrix M^{i}_{AB} for the motion of adjacent bodies A and B can be obtained by multiplying their initial position transformation matrix P_{AB}, the ideal motion transformation matrix T^{i}_{AB}, the initial position error transformation matrix ΔP_{AB}, and the ideal motion error transformation matrix ΔT_{AB}, as shown in Eqn. (2).

$$M^{i}_{AB} = P_{AB}\Delta P_{AB}T^{i}_{AB}\Delta T_{AB} \quad (2)$$

According to the topological structure of the machine tool, the machine can be divided into two workpiece chains and one tool chain, with the machine's axis as the base coordinate system. The first workpiece chain is: bed-A axis-workpiece; the second workpiece chain is: bed-U axis-B2 axis-workpiece; the tool chain is: bed-X axis-Y axis-Z axis-B axis-tool.

In the turning mode, the machine tool can perform rough turning, finish turning, thread cutting, and other processes for implant and abutment parts. The turning spindle drives the rod material to rotate, while the B-axis direct-drive rotary table is fixed in the Z direction. The spindle is locked, ensuring that the turning tool remains fixed without changing the tool's direction vector. The machine tool performs front machining through the first workpiece chain - tool chain, allowing five-axis simultaneous movement. It has multi-position machining capabilities for coaxial milling, orthogonal milling, and non-orthogonal milling. When performing back-side machining in milling mode through the second workpiece chain - tool chain, the rod material is first cut off by the tool, then the vise is flipped, and the machine enters the back-side machining mode. At this point, the machine tool can achieve four-axis simultaneous cutting motion. The ideal position vector, actual position vector, and error of the tool tip are shown in Tab. 1.

	Turning	First Workpiece Chain - Tool Chain Milling	Second Workpiece Chain - Tool Chain Milling

Ideal Position Vector of the Tool Tip	$M_{t1}^{i} = (M_{12}^{i}\ M_{23}^{i})^{-1}\ M_{14}^{i}$ $\cdot M_{45}^{i} M_{56}^{i} M_{67}^{i} M_{78}^{i} P_t$ $= (P_{12}\ P_{23})^{-1} P_{14}\ T_{14}^{i}\ P_{45}$ $\cdot T_{45}^{i}\ P_{56}\ T_{56}^{i}\ P_{67}\ P_{78}\ P_t$	$M_{t2}^{i} = (M_{12}^{i}\ M_{23}^{i})^{-1}\ M_{14}^{i} M_{45}^{i}$ $\cdot M_{56}^{i}\ M_{67}^{i}\ M_{78}^{i}\ P_t$ $= (P_{12}\ T_{12}^{i}\ P_{23}\ T_{23}^{i})^{-1} P_{14}$ $\cdot T_{14}^{i}\ P_{45}\ T_{45}^{i}\ P_{56}\ T_{56}^{i}$ $\cdot\ P_{67}\ T_{67}^{i}\ P_{78}\ T_{78}^{i}\ P_t$	$M_{t3}^{i} = (M_{19}^{i}\ M_{9(10)}^{i} M_{(10)3}^{i})^{-1}$ $\cdot M_{14}^{i}\ M_{45}^{i}\ M_{56}^{i}\ M_{67}^{i}\ M_{78}^{i}\ P_t$ $= (P_{19}\ T_{19}^{i}\ P_{9(10)} T_{9(10)}^{i} P_{(10)3} T_{(10)3}^{i})^{-1}$ $\cdot P_{14}\ T_{14}^{i}\ P_{45}\ T_{45}^{i}\ P_{56}$ $\cdot T_{56}^{i}\ P_{67}\ T_{67}^{i}\ P_{78}\ T_{78}^{i}\ P_t$
Actual Position Vector of the Tool Tip	$M_{t1}^{a} = (M_{12}^{a}\ M_{23}^{a})^{-1} M_{14}^{a}\ M_{45}^{a}$ $\cdot M_{56}^{a}\ M_{67}^{a}\ M_{78}^{a}\ P_t$ $= (P_{12}\ \Delta P_{12}\ \Delta T_{12}$ $\cdot P_{23}\ \Delta P_{23}\ \Delta T_{23})^{-1}$ $\cdot P_{14}\ \Delta P_{14}\ T_{14}^{i}\ \Delta T_{14}$ $\cdot P_{45}\ \Delta P_{45}\ T_{45}^{i}\ \Delta T_{45}$ $\cdot P_{56}\ \Delta P_{56}\ T_{56}^{i}\ \Delta T_{56}$ $\cdot P_{67}\ \Delta P_{67}\ \Delta T_{67}\ P_{78}$ $\cdot \Delta P_{78}\ \Delta T_{78}\ P_t$	$M_{t2}^{a} = (M_{12}^{a} M_{23}^{a})^{-1}\ M_{14}^{a} M_{45}^{a}$ $\cdot M_{56}^{a} M_{67}^{a} M_{78}^{a} P_t$ $= (P_{12}\ \Delta P_{12}\ T_{12}^{i}\ \Delta T_{12}$ $\cdot P_{23}\ \Delta P_{23}\ T_{23}^{i}\ \Delta T_{23})^{-1}$ $\cdot P_{14}\ \Delta P_{14}\ T_{14}^{i}\ \Delta T_{14}$ $\cdot P_{45}\ \Delta P_{45}\ T_{45}^{i}\ \Delta T_{45}$ $\cdot P_{56}\ \Delta P_{56}\ T_{56}^{i}\ \Delta T_{56}$ $\cdot P_{67}\ \Delta P_{67}\ T_{67}^{i}\ \Delta T_{67}$ $\cdot P_{78}\ \Delta P_{78}\ T_{78}^{i}\ \Delta T_{78}\ P_t$	$M_{t3}^{a} = (M_{19}^{a} M_{9(10)}^{a} M_{(10)3}^{a})^{-1}$ $\cdot M_{14}^{a} M_{45}^{a} M_{56}^{a} M_{67}^{a} M_{78}^{a} P_t$ $= (P_{19}\ \Delta P_{19}\ T_{19}^{i}\ \Delta T_{19}\ P_{9(10)}$ $\cdot \Delta P_{9(10)} T_{9(10)}^{i} \Delta T_{9(10)} P_{(10)3}$ $\cdot \Delta P_{(10)3} T_{(10)3}^{i}\ \ \Delta T_{(10)3})^{-1}$ $\cdot P_{14}\ \Delta P_{14}\ T_{14}^{i}\ \Delta T_{14}\ P_{45}$ $\cdot \Delta P_{45}\ T_{45}^{i}\ \Delta T_{45}\ P_{56}\ \Delta P_{56}$ $\cdot T_{56}^{i}\ \Delta T_{56}\ P_{67}\ \Delta P_{67}\ T_{67}^{i}$ $\cdot \Delta T_{67}\ P_{78}\ \Delta P_{78}\ T_{78}^{i}\ \Delta T_{78}\ P_t$
Error	$\Delta E_{t1} = M_{t1}^{a} - M_{t1}^{i}$	$\Delta E_{t2} = M_{t2}^{a} - M_{t2}^{i}$	$\Delta E_{t3} = M_{t3}^{a} - M_{t3}^{i}$

Tab. 1: Ideal position vector of the tool tip, actual position vector of the tool tip, and error.

In the equation, P_t represents the position vector of the tool tip in the tool coordinate system, P_t= (P_{TX}, P_{TY}, P_{TZ}, 1) ^{T}, P_{TX}, P_{TY}, P_{TZ} represent the coordinate values of the tool tip along the three coordinate axes, which vary depending on the tool.

Precision Allocation

The impact of each error source on the output error varies. Sensitivity analysis of the error sources can identify the significant influencing errors of the machine tool, providing a basis for precision allocation of the machine tool components. According to the representation of the first-order sensitivity function, the sensitivity of the error terms in each direction of the machine tool can be expressed as Eqn. (3).

$$S_{ij}^{m} = \frac{\partial E_m}{\partial E_{ij}} \tag{3}$$

In the equation, m represents the direction, taking values x, y, and z; E_{ij} is the error source; and S_{ij}^{m} is the sensitivity of the error term E_{ij} in the m-direction error component.

The dimensional units of the error sensitivities of the machine tool are not consistent, making direct analysis and comparison difficult. Therefore, a normalization process is first performed. The sum of the sensitivity coefficients of the error components in each direction is set to 1. This allows for the direct identification of key error elements based on the sensitivity parameter values.

To identify the error factors that have a significant impact on the part machining dimensions, five key machining points are selected based on the machining process of the part: coaxial turning point, coaxial milling point, part cutting point, A-axis rotation machining point, and abutment angle curved surface machining point. The straightness error is set to 0.1, and the perpendicularity and angular errors are set to 0.1. The feed values of each axis and the coordinates of the tool tip are input at these settings, and the geometric sensitivity values are calculated. This allows for the identification of the main geometric errors in the model and the analysis of the patterns.

In this study, the error sensitivity was calculated by selecting five key points. Regardless of the machining mode of the machine tool, the errors primarily manifest as perpendicularity errors and angular errors, while straightness errors and positioning errors can be considered negligible. The perpendicularity error consistently represents the largest proportion among all the machine tool errors,

so it should be the first to be controlled for precision. Next, the angular error weight is considered, and precision allocation is performed for the other corresponding errors. We summarize the errors at each characteristic point and, based on the sensitivity values along the coordinate axes, define as key error elements those errors whose single sensitivity coefficient exceeds 0.05 and whose accumulated sensitivity parameter reaches the top 95% of the errors. This serves as the guideline for precision design.

Manufacturing Process Generation:

Dental implant components, such as implants and abutments, can be divided into two categories: general-purpose and personalized. Among them, general-purpose parts have already formed a series of standardized products. Therefore, these standardized products can be grouped into a part family, and the process templates for the part family can be constructed. This allows new parts to quickly generate their manufacturing process by searching for and reusing the process templates. The process mainly consists of two parts: process template construction and process template matching: (1) summarize the geometric and process characteristics of various parts, such as implants and abutments, to construct a process template library that stores process parameter information. (2) for new parts, the manufacturing process can be quickly generated through process template matching, thus improving programming efficiency and shortening process preparation time.

Process Template Construction

The core of the process template is to transform process data into a structured representation that associates geometry with process information. This paper constructs a geometric-process association model with manufacturing features as the core. The model includes geometric element information used to constrain and describe feature shapes, manufacturing semantic information related to manufacturing requirements, and process information associated with the manufacturing activities of the feature. Manufacturing semantics refer to the basic attributes of the feature, such as material, surface roughness, tolerance, etc., which are attached to the processing geometry. Geometric parameters include characteristics such as radius, area, height, and other related measurements.

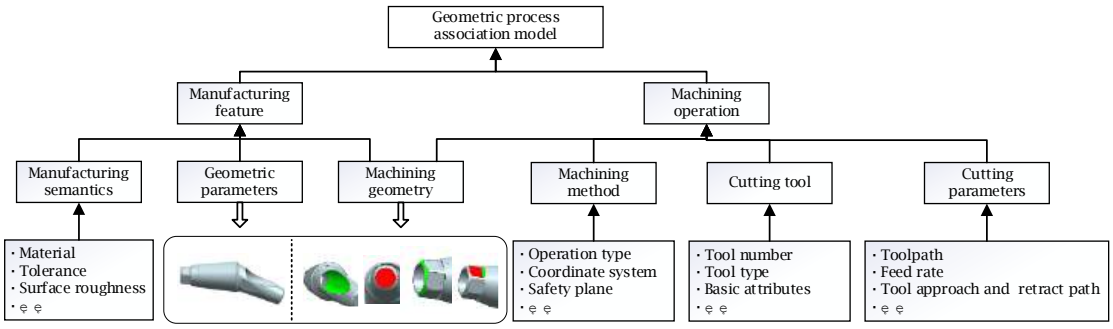

Fig. 5: Geometric-process association model.

Traditionally, process templates are derived from the experience and summarization of process personnel. After constructing the manufacturing feature process information model, the relationships between process elements are effectively represented. Process templates can be obtained through data mining. The specific approach is as follows: First, associate the accumulated part process routes in the enterprise with the manufacturing feature attribute information obtained through analysis (such as feature type, depth, diameter, area, maximum/minimum width, geometric tolerances, dimensional tolerances). Then, use the multi-dimensional similarity calculation results between different process routes as an important basis for clustering and classification. The data is processed through clustering, and ultimately, processed route templates are obtained and stored in the system database.

Process Template Matching

In process data, manufacturing features primarily include basic manufacturing features (such as holes, grooves, and end faces). During the manufacturing feature matching process, only manufacturing features with consistent feature types have reuse value. Each type of feature has its own key parameters. For features of the same type, differences in geometric parameters such as hole diameter, depth, corner radius, and maximum/minimum width can result in different reuse values. In the process design, dimensional tolerances, geometric tolerances, and roughness processing methods are closely related. For two manufacturing features with exactly the same geometric shape, if the precision requirements differ significantly, their corresponding processing technologies may be quite different. Based on process knowledge, the matching degree of the manufacturing process is evaluated by calculating the similarity of three factors: feature type, geometric parameters, and precision requirements. The specific calculation method is shown in Tab. 2.

Feature Type	Geometric Parameters	Precision Requirements
$S_T = \begin{cases} 0, & T_1 \neq T_2 \\ 1, & T_1 = T_2 \end{cases}$	$S_P = \sum_{i=0}^{n} \frac{1}{n} \times S_p(i)$	$S_A = \frac{1}{3} \times (S_{DIM} + S_{FP} + S_{RO})$

Tab 2: Calculation method for similarity of feature type, geometric parameters, and precision requirements.

In the formula, S_T represents the feature similarity, T represents the feature, S_P represents the similarity of geometric parameter matching, n represents the number of geometric parameters, $S_p\ (i)$ represents the similarity of the i geometric parameter matching, S_A represents the similarity of accuracy requirements, SDIM represents the similarity of dimensional tolerances, S_{FP} represents the similarity of geometric tolerances. S_{RO} represents the similarity of roughness, and the values of S_{DIM}, S_{FP} and S_{RO} are 0 or 1. The similarity of the feature information associated with the new part manufacturing feature and the feature process template is defined as the weighted sum of the similarity of the manufacturing feature type, the geometric parameter, and the accuracy requirement. It is represented by δ, and the feature template with the highest similarity is taken as the feature process template of the manufacturing feature to be manufactured.

$$\delta = \begin{cases} \frac{S_T + S_P + S_A}{3}, S_T = 1 \\ 0 \qquad\quad , S_T = 0 \end{cases} \tag{4}$$

Process template matching is to match the feature information in the process template with the feature information of the parts to be manufactured (new parts), and infer the process template of the parts to be manufactured (new parts). Firstly, feature matching is performed, and the logarithm m of the matched correlation features and the similarity δ of each pair of matching features are output. By calculating the similarity value between the manufacturing features of new parts and the associated features in all process templates, the process template with the highest similarity value is used as the process route of new parts, and the process plan is generated. The similarity between the new part and the process route template is represented as S_{TM}, as shown in the following Eqn. 5.

$$S_{TM} = \frac{1}{m} \sum_{i=0}^{m} \frac{1}{\delta} \tag{5}$$

Finally, by calculating the S_{TM} values of the new part's manufacturing features with all the associated features in the process templates, the process template with the highest S_{TM} value is selected as the process route for the new part, and the corresponding process plan is generated.

Machining Process Control:

For small and complex parts like dental implants, their machining trajectories are often composed of spatial arcs and helical lines[5], which are geometries that can be precisely and rapidly interpolated. In the NC machining process of such parts, CAD-designed spatial curves are discretized into numerous

small line segments, ultimately generating CNC programs consisting of many G01 commands. To reduce the data size of the NC code, improve the machining efficiency and quality of the workpiece, this paper proposes a spiral trajectory smoothing compression algorithm specifically tailored to the machining characteristics of dental implants. This algorithm smooths and compresses the incoming small line segments, converting the polyline machining path, composed of numerous discrete small segments, into a smooth machining path. This approach significantly optimizes the machining process by reducing computational load, enhancing toolpath accuracy, and improving overall machining efficiency.

Spiral Trajectory Smoothing Compression Algorithm

The basic idea of the Spiral Trajectory Smoothing Compression Algorithm is: by performing two fittings in the XY plane and along the Z-axis direction, the algorithm distinguishes between straight lines, arcs, and spatial spirals, achieving global smoothing of small tool trajectory segments. Then, ahead velocity planning is applied between each segment of the curve to ensure smoothness of overall speed, thus achieving efficient and high-quality processing of dental implants. The proposed fitting scheme includes three steps: plane fitting, curve classification, and spatial spiral fitting.

This paper uses the Pratt arc fitting method[6] to implement a plane fitting approach that approximates the projection of the tangent points onto the XY plane using arcs or straight lines. The Pratt method describes the equation of a circle as follows $A(x_i^2+y_i^2)+Bx_i+Cy_i+D=0$. By transforming the difference between $D=\sqrt{(x-a)^2+(y-b)^2}$ and the radius R into D^2-R^2, the nonlinear problem is converted into a linear one.

Another advantage of using the Pratt fitting method is that the equation incorporates the line equation. When the coefficient A = 0, the resulting curve becomes a straight line. Furthermore, in space, we classify the data by checking whether the coordinates of two consecutive trajectory points are increasing or decreasing along the tool vector direction. This helps distinguish between straight lines, planar arcs, and spiral lines. As a result, the tool path described by small line segments can be converted into larger straight line and arc segments, reducing the data size and improving both the overall machining efficiency and quality.

Fitting error control is an essential process during trajectory fitting. It not only determines the accuracy of the fitting algorithm but also plays a crucial role in ensuring that the curves before and after fitting meet the required standards. Generally speaking, calculating the deviation of a spatial curve is difficult. In this case, we decompose the spiral curve into a combination of circular motion and axial motion based on the characteristics of the spiral line formation. The error for each motion is then calculated separately.

Speed Feedforward Control

The specialized machining equipment in this paper uses an open CNC system based on GTS. The input NC program is sent to the data feedforward buffer after being processed by the program preprocessing module. The system first identifies deceleration characteristics and detects velocity change points in the processing path based on corner constraints. Then, based on the mechanical performance and other constraints of the machining center, the maximum allowable speed and maximum allowable acceleration of the machining center are determined. Using speed and acceleration as constraints, the system evaluates whether deceleration is required.

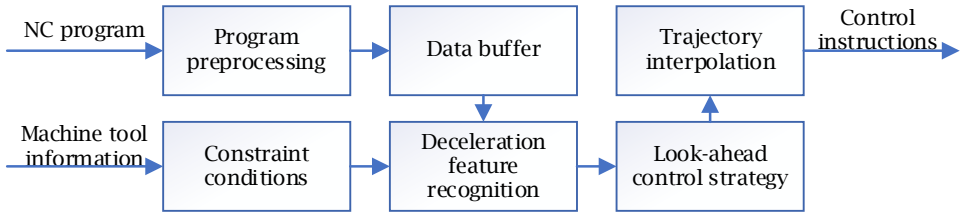

Fig. 6: Feedforward control implementation principle.

In the GTS motion controller, the multi-axis feedforward module is an independent functional module that automatically optimizes the overall motion speed of the trajectory during the processing of numerous continuous small line segments. This method is currently the most practical solution to improve machining efficiency and quality, which are often reduced due to frequent acceleration and deceleration caused by small line segment machining trajectories. The feedforward preprocessing module is used to plan the speed, significantly enhancing the speed during the small line segment machining process.

Machining Experiment:

In order to verify the functionality and performance of the specialized machining equipment for oral implant medical devices, machining experiments were conducted using an implant with a threaded diameter of φ3.5 mm and a 15° angled abutment as the test objects, as shown in Fig. 7. A 12mm diameter 6061 aluminum alloy bar stock was selected as the workpiece blank, as shown in Fig. 7(c). The CAD model of the angled abutment was used for feature recognition, and 19 machining operations were generated, as shown in Fig. (b). During the machining process, the spiral trajectory smoothing and compression algorithm, as well as the speed feedforward control, were tested.

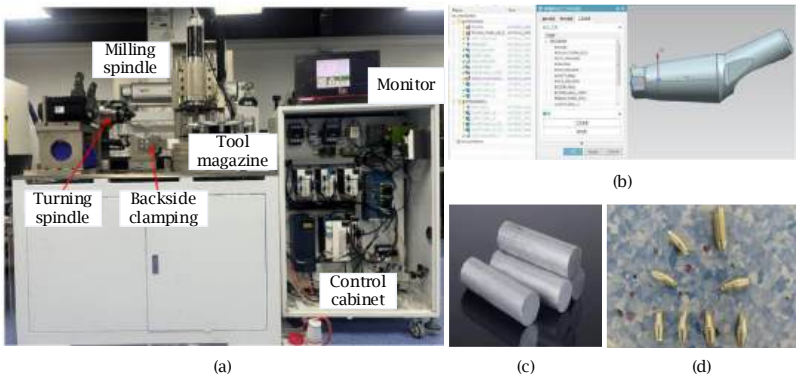

Fig. 7: (a) Physical image of the dedicated seven-axis turning and milling composite CNC machining center; (b) The process generation result of the angled abutments; (c) The physical image of the blank; (d) Sample part of dental implant device processing.

As shown in the figure, the actual processed dimensions of the part after machining are generally consistent with the standard parameters of the model base, meeting the accuracy requirements. Data from sensors indicate that the machining time using the spiral trajectory smoothing and compression method is significantly shorter compared to directly using small line segments, with machining time reduced by about 7% compared to using only the speed feedforward algorithm, thus improving overall operation speed. Therefore, this experiment successfully verified that the algorithm can indeed improve the machining efficiency of the parts. After multiple adjustments and experiments, functions such as turning, drilling, peck drilling, milling at arbitrary angles, and back machining were tested, and the results confirmed that the specialized machining equipment meets the required machining functions and performance.

Conclusions:

This paper developed a dedicated seven-axis machining equipment capable of fully automated processing for dental implant components such as implants and abutments. Meanwhile, the machine tool's structural design was optimized through error analysis and precision distribution. The proposed rapid generation method for NC machining processes reduces process preparation time. Additionally, the designed spiral trajectory smoothing and compression algorithm effectively improves the machining efficiency of the workpieces.

Acknowledgements:
The authors are grateful to the financial support from the Shenzhen Science and Technology Program (Grant No. RCBS20221008093056024, KJZD20230923114606013), the Guangdong Basic and Applied Basic Research Foundation (Grant No. 2024A1515012096).

References:
[1] Guo M.: Research and Application of Innovation-Driven Product Design. Shenyang：Shenyang University of Technology, 2016. (in Chinese)
[2] Chen X.S.; Xie L.H.; Chen J.Y.; Du R.X.; Deng F.L.: Design and fabrication of custom-made dental implants, Journal of Mechanical Science and Technology, 2012, 26(7), 1993-1998. Chen X.S.; Xie L.H.; Chen J.Y.; Du R.X.; Deng F.L.: Design and fabrication of custom-made dental implants, Journal of Mechanical Science and Technology, 2012, 26(7), 1993-1998. https://doi.org/10.1007/s12206-012-0501-9
[3] Liang J.M.; Zhou X.F.; Sun K.Z.; Chen X.S.: Development and Application of a PID Auto-Tuning Method to a CNC Servo Control, Applied Mechanics and Materials, 2014, 490, 897-901. https://doi.org/10.4028/www.scientific.net/AMM.490-491.897
[4] Chen X.S.; Zhang D.L.; Yuan S.M.; Zhang X.: A Precision CNC Turn-Mill Machining Center with Gear Hobbing Capability. Applied Mechanics and Materials, 2013, 300-301, 1241-1249. https://doi.org/10.1016/j.precisioneng.2014.09.006
[5] Cheng S.; Liu J.Q.; Zhou Z.R.; Huang Z.T.: Development of CNC System for Precision Roll Machine Tool. Machine Tools and Hydraulics, 2020, 48(10), 84-87. https://doi.org/10.3969/j.issn.1001-3881.2020.10.017
[6] Pratt, V.: Direct least-squares fitting of algebraic surfaces. ACM SIGGRAPH computer graphics, 21(4), 1987, 145-15. https://doi.org/10.1145/37401.37420